OPEN

Correspondence and
requests for materials
should be addressed to
W.T. (weitan@csrc.ac.
cn) or L.C. (cls@csrc.
ac.cn)

* These authors
contributed equally to
this work.

Photonic simulation of topological superconductor edge state and zero-energy mode at a vortex

Wei Tan[1]*, Liang Chen[1]*, Xia Ji[2]* & Hai-Qing Lin[1]

[1]Beijing Computational Science Research Center, Beijing 100084, China, [2]Academy of Mathematics and Systems Science, Chinese Academy of Sciences, Beijing 100190, China.

Photonic simulations of quantum Hall edge states and topological insulators have inspired considerable interest in recent years. Interestingly, there are theoretical predictions for another type of topological states in topological superconductors, but debates over their experimental observations still remain. Here we investigate the photonic analogue of the $p_x + ip_y$ model of topological superconductor. Two essential characteristics of topological superconductor, particle-hole symmetry and $p_x + ip_y$ pairing potentials, are well emulated in photonic systems. Its topological features are presented by chiral edge state and zero-energy mode at a vortex. This work may fertilize the study of photonic topological states, and open up the possibility for emulating wave behaviors in superconductors.

Topological state is a fundamentally new quantum state which is topologically distinct from all conventional states of matter. The first example is the quantum Hall (QH) state which has a full gap in the bulk and gapless chiral modes at the edge[1,2]. In the QH system, an external magnetic field is applied, explicitly breaking time-reversal (TR) symmetry. Beside this, another topological class of materials have been demonstrated invariant under TR, in the presence of strong spin-orbit coupling, which is named as topological insulator or quantum spin Hall (QSH) effect[3–7]. The QSH state in two dimension (2D) can be roughly understood as two copies of the QH state, where states with opposite spin propagate in opposite directions at the edge[7].

In 2008 Haldane and Raghu demonstrated the possibility of achieving photonic analogue of the QH edge states of electrons, based on the fact that the edge states are a property of a one-particle eigenstates problem, which can be mapped into the Maxwell normal-mode problem[8]. Such photonic edge states were soon realized in microwave experiments in photonic crystals made with magneto-optic media[9,10]. Since then, various configurations have been proposed to achieve photonic topological states, such as aperiodic coupled-resonator system[11] and dynamically modulated photonic resonator lattice exhibiting an effective magnetic field[12]. These topologically protected edge states ensure the absence of backscattering of waves by disorder, which suggest potential applications ranging from on-chip isolation[10] to delay line[11]. Meanwhile photonic simulations of topological insulator without the breaking of TR symmetry have been designed in photonic metacrystal made with bi-anisotropic media[13] and a lattice of optical ring resonators[14]. More recently, photonic Floquet topological insulator has been experimentally realized in a honeycomb lattice composed of coupled helical waveguides[15], and synthetic magnetic fields for photons have been achieved by using linear silicon photonics[16].

Interestingly, there is another type of topological states in chiral topological superconductor (TSC) which has a pairing gap in the bulk and gapless bound state at the edge[6,7]. Besides the edge state, the existence of zero-energy mode at a vortex core has been theoretically predicted[17,18], which attracts great attention in the recent decade[19]. The simplest model for the TR breaking TSC is proposed in $p_x + ip_y$ pairing states[17], whose Hamiltonian is given as[7]

$$\mathbf{H}_{\vec{p}} = \begin{bmatrix} \frac{p^2}{2m'} - U' & \Delta(p_x + ip_y) \\ \Delta^*(p_x - ip_y) & U' - \frac{p^2}{2m'} \end{bmatrix}, \qquad (1)$$

where $\vec{p}$ is the momentum, U' is the chemical potential, and the off-diagonal elements are pairing potentials. In the weak pairing phase with $U' > 0$, chiral edge states appear[7]. Although many attempts have been made to observe such edge states experimentally, there are still debates on them[20–23].

In this work, we bridge the fields of TSC and photonics. A direct mapping is established between the $p_x + ip_y$ Hamiltonian of TSC and the effective Hamiltonian of a suitably designed electromagnetic medium. Photonic simulations of TSC edge state and zero-energy mode at a vortex are investigated. This study extends the essential physics of the $p_x + ip_y$ model to photonic systems, which may provide a clean and convenient platform to study topological states of TSC, due to the flexibility of material design and less difficulties in experimental observations. On the other hand, this idea may fertilize the study of photonic topological states, and inspire researchers to explore more fruitful topological effects.

Results

Photonic analogue of the $p_x + ip_y$ Hamiltonian. The main challenges of achieving photonic analogue of the $p_x + ip_y$ Hamiltonian lie in two aspects: (i) one of the critical properties of TSC is particle-hole symmetry, of which the photonic counterpart may seem unimaginable at first sight; (ii) pairing potential of the $p_x + ip_y$ pairing state is required to be a linear function of momentum (see the off-diagonal elements of the Hamiltonian), whereas such kind of interaction is not common in electromagnetic media. Here we propose a two-step approach to give a solution.

In general, the propagating waves in 2D can be classified into transverse electric (TE) mode and transverse magnetic (TM) mode. Thanks to electromagnetic duality of Maxwell's equations, equations for TE mode can be converted into that for TM mode by making transformations of $E_z \rightarrow H_z$, $H_x \rightarrow -E_x$, $H_y \rightarrow -E_y$, $\varepsilon \rightarrow \mu$, and $\mu \rightarrow \varepsilon$. We suggest using band structures of TE and TM modes to mimic particle and hole states, respectively. However, electromagnetic duality is not enough for realizing photonic "particle-hole symmetry", since particle-hole transformation also changes the sign of the kinetic energy. We design photonic band structures with positive- and negative-refractive-index bands by using metamaterials[24–29], which are also known as right-handed and left-handed bands, to mimic the positive- and negative-energy bands of particle and hole, respectively. In this way, the particle-hole transformation in condensed matter physics is emulated by a combination of electromagnetic duality and handedness inversion in photonics, as schematically shown in figure 1a. For example, a right-handed TE band and a well-designed left-handed TM band can present photonic "particle-hole symmetry".

Reference 29 demonstrated that one-dimensional (1D) Maxwell's equations can be transformed into a compact form that has the identical mathematical structure of the Dirac equation. By employing metamaterials having controllable dispersive permittivity and permeability, a simple two-band model was achieved, including an upper right-handed band and a lower left-handed band. Here, we extend this idea to 2D Maxwell's equations. Take for example the TE mode, the time-harmonic Maxwell's equations in k-space can be written as

$$\begin{bmatrix} -(\omega/c)\varepsilon_z & -k_x & k_y \\ -k_x & -(\omega/c)\mu_\perp & 0 \\ k_y & 0 & -(\omega/c)\mu_\perp \end{bmatrix} \begin{bmatrix} \sqrt{\varepsilon_0}E_z \\ \sqrt{\mu_0}H_y \\ \sqrt{\mu_0}H_x \end{bmatrix} = 0, \quad (2)$$

where ω is the angular frequency, c is the speed of light in vacuum, ε_0/μ_0 are the permittivity/permeability of the vacuum, $\varepsilon_z/\mu_\perp$ are the relative permittivity/permeability of the medium, k_x and k_y are propagation constants in the x and y direction, respectively. Consider suitably designed metamaterial whose effective permittivity and permeability are described by the Drude model,

$$\varepsilon_z = \varepsilon_{z0} - \frac{\omega_{pe}^2}{\omega^2 + i\omega\gamma_e}, \quad \mu_\perp = \mu_{\perp 0} - \frac{\omega_{pm}^2}{\omega^2 + i\omega\gamma_m}, \quad (3)$$

where ω_{pe}/ω_{pm} are the plasma/"magnetic plasma" frequency, γ_e/γ_m are losses, and $\varepsilon_{z0}/\mu_{\perp 0}$ are constants. For simplicity, we assume $\gamma_e = \gamma_m = 0$ and $\omega_{pe} = \omega_{pm} \equiv \omega_p$ in theoretical investigations. Let $\delta\varepsilon_z \equiv \varepsilon_{z0} - \omega_p^2/\omega_0^2$, and $\delta\mu_\perp \equiv \mu_{\perp 0} - \omega_p^2/\omega_0^2$, where ω_0 is a reference frequency that is chosen as the photonic analogue of zero energy of superconductor. As all interesting physics of TSC occur around zero energy, we focus on the vicinity of ω_0 accordingly and do expansions,

$$\omega\varepsilon_z \approx 2\omega_p^2\omega_0^2(\omega-\omega_0)+\omega\delta\varepsilon_z, \quad \omega\mu_\perp \approx 2\omega_p^2\omega_0^2(\omega-\omega_0)+\omega\delta\mu_\perp. \quad (4)$$

By substituting equation (4) into equation (2), we get

$$\begin{pmatrix} m-U & -k_x & k_y \\ -k_x & -m-U & 0 \\ k_y & 0 & -m-U \end{pmatrix} \begin{pmatrix} E_z' \\ H_y' \\ H_x' \end{pmatrix} = \Omega \begin{pmatrix} E_z' \\ H_y' \\ H_x' \end{pmatrix}, \quad (5)$$

where $E_z' = \sqrt{\varepsilon_0}E_z$, $H_{x,y}' = \sqrt{\mu_0}H_{x,y}$, m is the effective mass, $m = \omega(\delta\mu_\perp - \delta\varepsilon_z)/2c$, U is the effective chemical potential, $U = \omega(\delta\mu_\perp + \delta\varepsilon_z)/2c$, and Ω is the eigen-frequency, $\Omega = 2\omega_p^2\omega_0^2(\omega-\omega_0)$. The 3×3 matrix in the left-hand side of equation (5) can be considered as an effective Hamiltonian for TE mode, denoted by
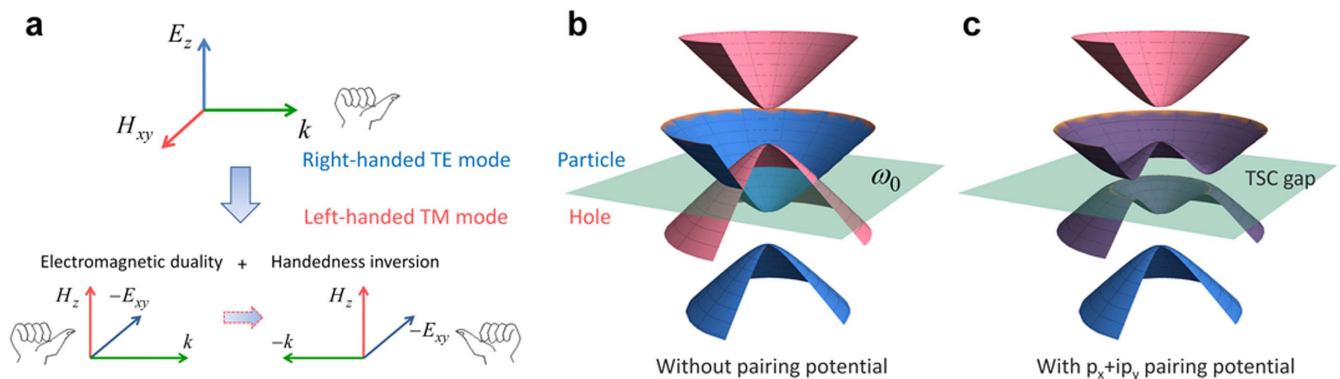

Figure 1 | Photonic simulation of TSC band structures. (a) A combination of electromagnetic duality and handedness inversion of photons mimics particle-hole transformation for electrons. For example, if a right-handed TE mode represent "particle", a transformed left-handed TM mode can be considered as "hole". (b,c) Band diagrams for particle-hole symmetric systems (b) without and (c) with $p_x + ip_y$ pairing potential. The $p_x + ip_y$ pairing potential leads to a gap with topological phase.

$$\mathbf{h}(\vec{k}) - U \equiv \begin{pmatrix} m-U & -k_x & k_y \\ -k_x & -m-U & 0 \\ k_y & 0 & -m-U \end{pmatrix}.$$

By tuning m and U, one can obtain a two-band diagram, as shown in figure 1b (colored blue).

Taking advantage of electromagnetic duality of Maxwell's equations, we can readily obtain the corresponding equations for TM mode from equation (2), which plays the role of "hole" state. Then we introduce handedness inversion, which flips the sign of permittivity and permeability. The material parameters are required to meet the conditions of $\delta\mu_z = -\delta\varepsilon_z \equiv -\delta_z$ and $\delta\varepsilon_\perp = -\delta\mu_\perp \equiv -\delta_\perp$. Consequently, the effective Hamiltonian of the TM mode is obtained, $-\mathbf{h}^*(-\vec{k}) + U$. The band diagram is plotted in figure 1b (colored pink). By tuning U to meet the condition $U > m$, the right-handed TE band and the left-handed TM band cross at a finite frequency, as shown in figure 1b. The crossing frequency is ω_0, which can be considered as photonic counterpart of zero energy in superconductor.

Next step is to emulate $p_x + ip_y$ pairing potential, which is responsible for a gap opening at ω_0. At first sight it might be very difficult to obtain photonic interaction that is a linear function of momentum. Here we introduce an alternative solution, which is named as odd-parity pairing[30,31]. In this picture, one can use constant interactions instead, if the interactions are applied between a wave function with odd parity and another with even parity. Note that for a single-orbital superconductor, odd-parity pairing is equivalent to p-wave pairing[30].

To achieve the photonic "odd-parity pairing", we introduce here the reflection operator M in 2D point groups[32,33]. Take for example the reflection M_x ($x \to -x$, $y \to y$) in the xy plane. Under this operation, k_x changes its sign ($k_x \to -k_x$). To keep Maxwell's equations invariant under M_x, we should have $H_y \to -H_y$ and $E_y \to -E_y$. Similar arguments can be applied to M_y. In contrast, for any reflection M in the xy plane, E_z and H_z keep their signs. In this picture, $E_{x,y}$ and $H_{x,y}$ act as "odd-parity" wave functions, while E_z and H_z act as "even-parity" wave functions. Therefore, we introduce interactions between E_z and $E_{x,y}$, and between H_z and $H_{x,y}$, respectively. We also notice that the required pairing potentials are expected for not only opening a gap but also breaking TR symmetry. As a result, the "odd-parity pairing" interactions are designed by employing complex off-diagonal elements in permittivity and permeability tensors,

$$\varepsilon = \begin{pmatrix} \varepsilon_\perp & 0 & \kappa_1 \\ 0 & \varepsilon_\perp & -i\kappa_2 \\ \kappa_1^* & i\kappa_2^* & \varepsilon_z \end{pmatrix}, \quad \mu = \begin{pmatrix} \mu_\perp & 0 & \kappa_3 \\ 0 & \mu_\perp & i\kappa_4 \\ \kappa_3^* & -i\kappa_4^* & \mu_z \end{pmatrix}. \quad (6)$$

Without loss of generality, we assume $\kappa_1 = \kappa_2 = \kappa_3 = \kappa_4 = \kappa$. In this case, the system has rotational symmetry in the $k_{x,y}$ plane.

After the above two steps, we obtain the effective Hamiltonian for the TSC-like photonic medium,

$$\mathbf{H}_{\text{eff}} = \begin{pmatrix} \mathbf{h}(\vec{k}) - U & \hat{\Delta} \\ -\hat{\Delta}^* & -\mathbf{h}^*(-\vec{k}) + U \end{pmatrix}, \quad \hat{\Delta} = \begin{pmatrix} 0 & i\Delta & \Delta \\ -i\Delta & 0 & 0 \\ -\Delta & 0 & 0 \end{pmatrix}, (7)$$

where $\Delta = \omega\kappa/c$. This Hamiltonian presents "particle-hole symmetry",

$$\Gamma\mathbf{H}_{\text{eff}}(k)\Gamma^\dagger = -\mathbf{H}_{\text{eff}}^*(-k), \quad \Gamma = \begin{pmatrix} 0 & \mathbf{1} \\ \mathbf{1} & 0 \end{pmatrix}. \quad (8)$$

The pairing potential $\hat{\Delta}$ results in a TSC-like gap centered at ω_0, as shown in figure 1c. To verify the topological feature of the TSC-like medium, we analytically calculate the winding number. It is known

that topological nature of a system changes only when the gap closes. This property enables us to investigate topological feature in the extreme case that the gap has nearly zero width. Here we use a general method of approximation for this problem. First, consider the case of absent pairing potential, as shown in figure 1b. The eigen-functions can be obtained by diagonalizing the 6×6 Hamiltonian described by equation (7). As all interesting physics are determined by the bands crossing zero energy, one may extract the 6×2 eigen-functions for the corresponding two bands and project out the others. Next, we open an extremely small gap by introducing a very weak pairing potential. An appropriate approximation is used here: for sufficiently small variation of k, treat this term as a perturbation, so as to get an expression for the Hamiltonian in terms of the gapless solutions. Consequently, we use the 6×2 eigen-functions of the gapless solutions to extract the 2×2 sub-matrix of the pairing case approximately,

$$H'_{\text{eff}} = \begin{pmatrix} \sqrt{m^2 + k_x^2 + k_y^2} - U & \dfrac{-i\Delta(k_x + ik_y)}{\sqrt{m^2 + k_x^2 + k_y^2}} \\ \dfrac{i\Delta(k_x - ik_y)}{\sqrt{m^2 + k_x^2 + k_y^2}} & U - \sqrt{m^2 + k_x^2 + k_y^2} \end{pmatrix} \quad (9)$$

$$\equiv d_x\sigma_x + d_y\sigma_y + d_z\sigma_z,$$

where $\sigma_{x,y,z}$ are the Pauli matrices. It can be directly mapped into the $p_x + ip_y$ TSC Hamiltonian described by equation (1). From equation (9), one can calculate the winding number analytically,

$$N_{\text{w}} = \frac{1}{4\pi} \int dk_x \int dk_y \hat{\mathbf{d}} \cdot \frac{\partial\hat{\mathbf{d}}}{\partial k_x} \times \frac{\partial\hat{\mathbf{d}}}{\partial k_y}. \quad (10)$$

In the present model, it gives $N_{\text{w}} = \theta(|U| - |m|) = 1$, providing a direct evidence for the topological phase.

Simulation of TSC edge state. The non-zero winding number promises a chiral edge state localized at the interface between the TSC-like medium and another opaque medium. Let the interface be at $x = 0$, and the opaque medium be located in the region $x < 0$. The dispersion relation of the edge state is illustrated by the red line in figure 2a, where the shaded areas indicate the projected band diagram of infinite TSC-like medium. The material parameters of the TSC-like medium are taken as $\varepsilon_{\perp 0} = 0.8, \varepsilon_{z0} = 1.1, \mu_{\perp 0} = 1.2, \mu_{z0} = 0.9$, (which lead to $\delta\varepsilon_\perp = -\delta\mu_\perp = -0.2, \delta\varepsilon_z = -\delta\mu_z = 0.1$), $\omega_p = 89$, and $\kappa = 0.04$ (with the unit of GHz). These parameters ensure the particle-hole-like symmetry of the effective Hamiltonian. From figure 2a, one can see a single branch of edge state with positive group velocity, which suggests broken TR symmetry and is expected to support one-way propagation. Note that another branch with negative group velocity can be realized by changing the permittivity and permeability tensors described by equation (6) into their conjugations, which makes the winding number flip its sign. To demonstrate the edge state intuitively, we also perform numerical calculations in real space by employing finite-difference frequency-domain (FDFD) method. As shown in figure 2b, the edge state distributes almost uniformly along the interface between two media and can pass through sharp bends at the corner without scattering.

One may question that the material parameters described by equation (6) with certain symmetries might be very difficult to be realized. Fortunately, it is known that topological nature of a system would not change if the gap doesn't close, and thus the edge state is topologically protected and insensitive to small perturbations. Taking advantage of this property, the strict requirements for material parameters with four pairs of off-diagonal elements could be reduced. Here, we remove two of them by letting $\kappa_2 = \kappa_3 = 0$ in equation (6), and perturb the symmetric Drude parameters of permittivity and per-
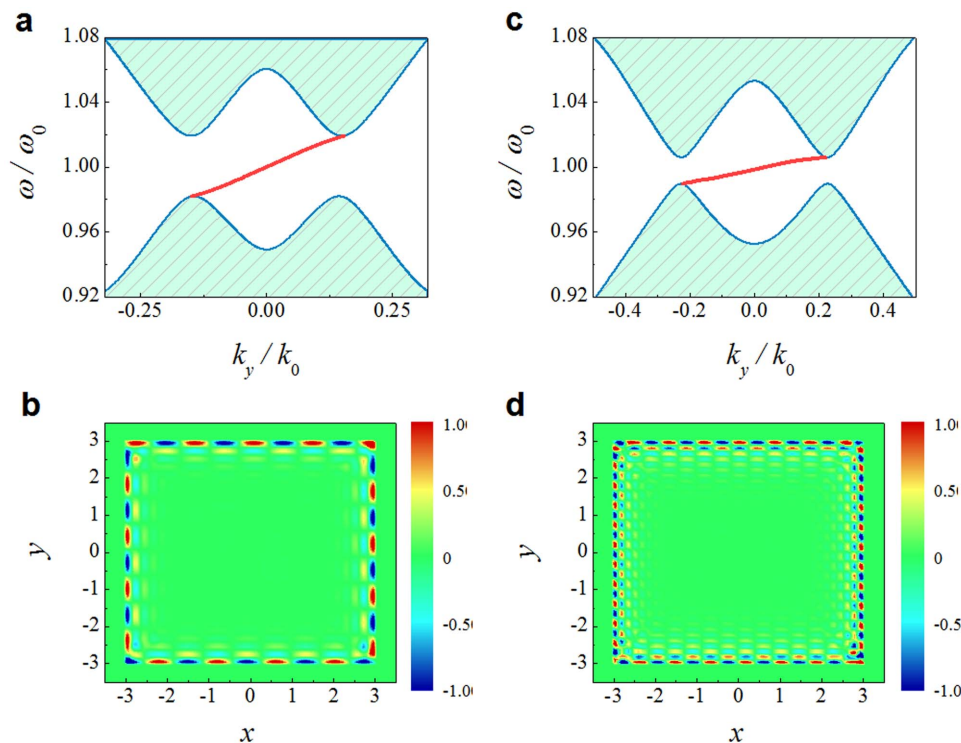
Figure 2 | Manifestation of chiral edge state in both reciprocal and real space. (a,b) Perfect analogy of TSC Hamiltonian and edge state with ideal material parameters. (a) Projected band diagram of infinite TSC-like photonic structure (shaded areas) and edge state at the interface between a semi-finite TSC-like medium in the region $x > 0$ and a semi-finite opaque medium in the region $x < 0$ (red line). (b) Magnetic field (H_z) distributions of edge state for a finite TSC-like medium. (c,d) Non-perfect TSC-like edge state with reduced material parameters. The results in (a) and (c) are analytically calculated by solving Maxwell's equations, and those in (b) and (d) are numerically simulated by employing FDFD method.

meability, for example, $\varepsilon_\perp = 2 - 140^2/\omega^2$, $\varepsilon_z = 2 - 121^2/\omega^2$, $\mu_\perp = 1 - 77^2/\omega^2$, $\mu_z = 1 - 94^2/\omega^2$, $\kappa_1 = 0.08$, and $\kappa_2 = 0.04$ (with the unit of GHz). In this case, the perfect form of the TSC-like Hamiltonian described by equation (7) no longer remains, and the band structure adiabatically deforms from the symmetric one without gap closing. Compared with figures 2a and 2c, the bulk gap in figure 2c is narrower, and the edge state in figure 2d shows broken rotational symmetry in the $k_{x,y}$ plane (the wavelength along the y direction is shorter than that along the x direction). Nevertheless, the edge state still exists. It provides an evidence for the topologically protected edge state against material-parameter perturbations, which may facilitate experimental realizations.

Simulation of zero-energy mode at a vortex. Another prominent feature of $p_x + ip_y$ superconductor is zero-energy mode at a vortex[17,34–37]. It is a solution of the Bogoliubov-de Gennes (BdG) equation in polar coordinates with $\Delta(r,\theta) = \Delta_0(r)\exp(\pm i\theta)$, characterized by a bound state at zero energy at a vortex core which can be roughly considered as a small circular edge with vanishing density at the center[17]. Zero-energy mode is another important topological excitation, but earlier works in photonics only concentrated on edge states. Here we introduce azimuth-dependent off-diagonal elements in permittivity and permeability tensors with cylindrical symmetry, for example, $\kappa_1 = \kappa_2 = \kappa \exp(-i\theta)$ and $\kappa_3 = \kappa_4 = \kappa \exp(+i\theta)$. This design mimics a counter-clockwise vortex with a singularity at the center. FDFD method is employed to numerically calculate the field distributions in a finite medium at zero energy (ω_0). The results are shown in figure 3. Two types of bound states are clearly seen: one appears at the edge and the other locates at the center "vortex core". We have also confirmed that the bound state at the vortex only exists at ω_0, which is indeed a "zero-energy" mode. It is known that the zero-energy modes at the vortex and at the edge can be described as the

Jackiw-Rebbi solution in the 1D Dirac equation at the domain wall[38,39]. Here we reproduce them in photonic structures. Further calculations illustrate that the mode around the center rotates counter-clockwise around the vortex core, while the other rotates clockwise along the edge. The electric and magnetic fields also show different patterns between these two modes: in one mode E_z and H_z oscillate in phase, while in the other E_z and H_z oscillate out of phase.

Discussion

It should be pointed out that the effective TSC Hamiltonian proposed in this work is based on the presence of complex off-diagonal elements in permittivity and permeability tensors, which can be brought by gyrotropic responses of materials. We note that in the past decade, the study of metamaterials has made remarkable progress in tailoring ε and μ of an effective medium, offering flexible ways for manipulating electromagnetic wave propagation, such as cloaking[40,41], optical analogue of quantum interference[42] and Fano resonance[43], and also mimicking black hole[44]. Most recently, the increased interests in achieving topological phases and edge states in photonic systems suggest that the presence of gyrotropic and chiral responses in materials may lead to fruitful results[8–13], and some of them have already been realized in experiments[10,15,45]. For more complicated cases, such as the vortex model in this work, position-dependent gyrotropic parameters are taken into account. It may inspire researchers to tailor gyrotropic responses of materials as well as ε and μ in the future.

In summary, we have established a direct mapping between the $p_x + ip_y$ model of topological superconductor and suitably designed electromagnetic medium. Two essential points of this mapping, particle-hole symmetry and $p_x + ip_y$ pairing, have been investigated in detail. A combination of electromagnetic duality and handedness inversion of photons was proposed to mimic particle-hole trans-
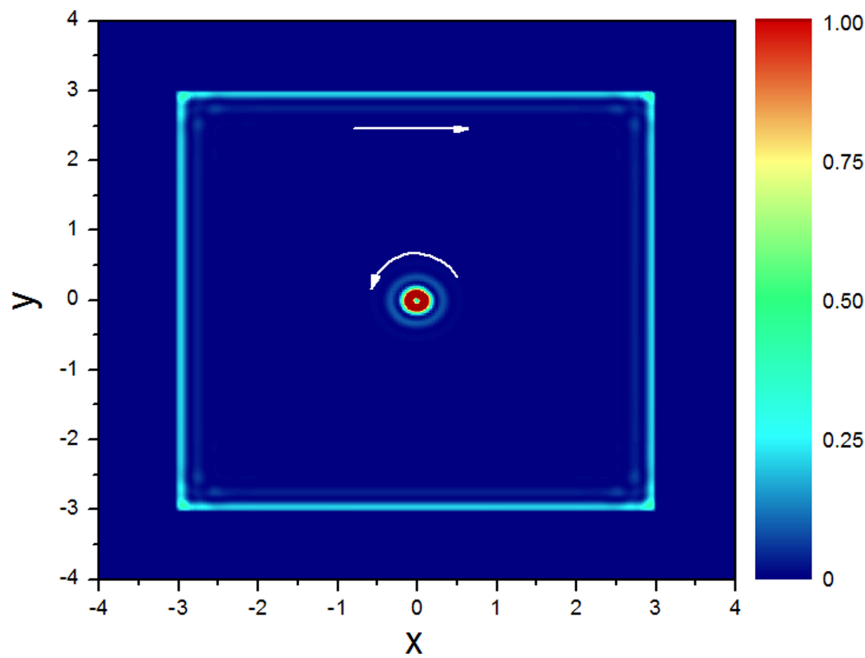
Figure 3 | Manifestation of photonic zero-energy modes at a vortex and at edges. The mode at the vortex propagates counter-clockwise around the center vortex core, while the mode at the edge propagates clockwise. Azimuth-dependent off-diagonal elements in permittivity and permeability tensors are introduced to mimic a vortex with a singularity at the center.

formation for electrons. The analogous $p_x + ip_y$ pairing potentials are achieved by introducing complex off-diagonal elements in permittivity and permeability tensors. Finally, we obtained a 2×2 effective Hamiltonian that has the identical mathematical structure of the TSC Hamiltonian, and mimicked TSC edge state and zero-energy mode at a vortex. This study bridges the fields of superconductor and photonics, providing a good platform for simulating wave behaviors in superconductor physics at room temperature. The $p_x + ip_y$ model for TSC is the first example, and other interesting effects such as Andreev reflection will be further investigated.

Methods

Band dispersions of both bulk media and edge states were obtained by analytically solving Maxwell's equations with effective permittivity and permeability. The effective Hamiltonian of the proposed photonic structures and its mapping into the $p_x + ip_y$ model of topological superconductor were carried out by theoretical deduction under appropriate approximations. Winding number was calculated analytically from the effective Hamiltonian. Numerical simulations were performed by using FDFD method.

1. Thouless, D. J. *et al.* Quantum Hall conductance in a two-dimensional periodic potential. *Phys. Rev. Lett.* **49**, 405–408 (1982).
2. Hatsugai, Y. Chern number and edge states in the integer quantum Hall effect. *Phys. Rev. Lett.* **71**, 3697–3700 (1993).
3. Kane, C. L. & Mele, E. J. Quantum spin Hall effect in graphene. *Phys. Rev. Lett.* **95**, 226801 (2005).
4. Bernevig, B. A. & Zhang, S. C. Quantum spin Hall effect. *Phys. Rev. Lett.* **96**, 106802 (2006).
5. Bernevig, B. A., Hughes, T. L. & Zhang, S. C. Quantum spin Hall effect and topological phase transition in HgTe quantum wells. *Science* **314**, 1757 (2006).
6. Hasan, M. Z. & Kane, C. L. Topological insulators. *Rev. Mod. Phys.* **82**, 3045 (2010).
7. Qi, X. L. & Zhang, S. C. Topological insulators and superconductors. *Rev. Mod. Phys.* **83**, 1057 (2011).
8. Haldane, F. D. M. & Raghu, S. Possible realization of directional optical waveguides in photonic crystals with broken time-reversal symmetry. *Phys. Rev. Lett.* **100**, 013904 (2008).
9. Wang, Z., Chong, Y., Joannopoulos, J. D. & Soljacic, M. Reflection-free one-way edge modes in a gyromagnetic photonic crystal. *Phys. Rev. Lett.* **100**, 013905 (2008).
10. Wang, Z., Chong, Y., Joannopoulos, J. D. & Soljacic, M. Observation of unidirectional backscattering-immune topological electromagnetic states. *Nature* **461**, 772–775 (2009).
11. Hafezi, M., Demler, E. A., Lukin, M. D. & Taylor, J. M. Robust optical delay lines with topological protection. *Nature Phys.* **7**, 907–912 (2011).
12. Fang, K., Yu, Z. & Fan, S. Realizing effective magnetic field for photons by controlling the phase of dynamic modulation. *Nature Photon.* **6**, 782–787 (2012).
13. Khanikaev, A. B. *et al.* Photonic topological insulators. *Nature Mater.* **12**, 233–239 (2012).
14. Liang, G. Q. & Chong, Y. D. Optical resonator analog of a two-dimensional topological insulator. *Phys. Rev. Lett.* **110**, 203904 (2013).
15. Rechtsman, M. C. *et al.* Photonic Floquet topological insulators. *Nature* **496**, 196–200 (2013).
16. Hafezi, M. *et al.* Imaging topological edge states in silicon photonics. *Nature Photon.* **6**, 782–787 (2013).
17. Read, N. & Green, D. Paired states of fermions in two dimensions with breaking of parity and time-reversal symmetries and the fractional quantum Hall effect. *Phys. Rev. B* **61**, 10267 (2000).
18. Ivanov, D. A. Non-Abelian statistics of half-quantum vortices in p-wave superconductors. *Phys. Rev. Lett.* **86**, 268 (2001).
19. Nayak, C. *et al.* Non-Abelian anyons and topological quantum computation. *Rev. Mod. Phys.* **80**, 1083 (2008).
20. Sasaki, S. *et al.* Topological superconductivity in $Cu_xBi_2Se_3$. *Phys. Rev. Lett.* **107**, 217001 (2011).
21. Hsieh, T. H. & Fu, L. Majorana fermions and exotic surface Andreev bound states in topological superconductors: Application to $Cu_xBi_2Se_3$. *Phys. Rev. Lett.* **108**, 107005 (2012).
22. Levy, N. *et al.* Experimental evidence for s-wave pairing symmetry in superconducting $Cu_xBi_2Se_3$ single crystals using a scanning tunneling microscope. *Phys. Rev. Lett.* **110**, 117001 (2013).
23. Peng, H. *et al.* Absence of zero-energy surface bound states in $Cu_xBi_2Se_3$ studied via Andreev reflection spectroscopy. *Phys. Rev. B* **88**, 024515 (2013).
24. Smith, D. R. *et al.* Composite medium with simultaneously negative permeability and permittivity. *Phys. Rev. Lett.* **84**, 4184–4187 (2000).
25. Shelby, R. A., Smith, D. R. & Schultz, S. Experimental verification of a negative index of refraction. *Science* **292**, 77–79 (2001).
26. Smith, D. R., Pendry, J. B. & Wiltshire, M. C. K. Metamaterials and negative refractive index. *Science* **305**, 788–792 (2004).
27. Li, J., Zhou, L., Chan, C. T. & Sheng, P. Photonic band gap from a stack of positive and negative index materials. *Phys. Rev. Lett.* **90**, 083901 (2003).
28. Jiang, H. *et al.* Properties of one-dimensional photonic crystals containing single-negative materials. *Phys. Rev. E* **69**, 066607 (2004).
29. Tan, W., Sun, Y., Chen, H. & Shen, S. Q. Photonic simulation of topological excitations in metamaterials. *Sci. Rep.* **4**, 3842; DOI:10.1038/srep03842 (2014).
30. Fu, L. & Berg, E. Odd-parity topological superconductors: theory and application to $Cu_xBi_2Se_3$. *Phys. Rev. Lett.* **105**, 097001 (2010).
31. Sato, M. Topological odd-parity superconductors. *Phys. Rev. B* **81**, 220504(R) (2010).
32. Liu, X., Hsu, H. C. & Liu, C. X. In-plane magnetization-induced quantum anomalous Hall effect. *Phys. Rev. Lett.* **111**, 086802 (2013).

33. Fang, C., Gilbert, M. J. & Bernevig, B. A. Bulk topological invariants in noninteracting point group symmetric insulators. *Phys. Rev. B* **86**, 115112 (2012).
34. Ivanov, D. A. Non-Abelian Statistics of Half-Quantum Vortices in p-wave superconductor. *Phys. Rev. Lett.* **86**, 268–271 (2001).
35. Stone, M. & Chung, S. B. Fusion rules and vortices in $p_x + ip_y$ superconductors. *Phys. Rev. B* **73**, 014505 (2006).
36. Sato, M. & Fujimoto, S. Topological phases of noncentrosymmetric superconductors: Edge states, Majorana fermions, and non-Abelian statistics. *Phys. Rev. B* **79**, 094504 (2009).
37. Mizushima, T. & Machida, K. Vortex structures and zero-energy states in the BCS-to-BEC evolution of -wave resonant Fermi gases. *Phys. Rev. A* **81**, 053605 (2010).
38. Jackiw, R. & Rebbi, C. Solitons with fermion number ½. *Phys. Rev. D* **13**, 3398 (1976).
39. Tewari, S., Sarma, S. D. & Lee, D. H. Index theorem for the zero modes of Majorana fermion vortices in chiral p-wave superconductors. *Phys. Rev. Lett.* **99**, 037001 (2007).
40. Leonhardt, U. Optical conformal mapping. *Science* **312**, 1777–1780 (2006).
41. Pendry, J. B., Schurig, D. & Smith, D. R. Controlling electromagnetic fields. *Science* **312**, 1780–1782 (2006).
42. Papasimakis, N., Fedotov, V. A., Zheludev, N. I. & Prosvirnin, S. L. Metamaterial analog of electromagnetically induced transparency. *Phys. Rev. Lett.* **101**, 253903 (2008).
43. Luk'yanchuk, B. *et al.* The Fano resonance in plasmonic nanostructures and metamaterials. *Nat. Mater.* **9**, 707–715 (2010).
44. Genov, D. A., Zhang, S. & Zhang, X. Mimicking celestial mechanics in metamaterials. *Nat. Phys.* **5**, 687–692 (2009).
45. Chen, W. J. *et al.* Experimental realization of photonic topological insulator in a uniaxial metacrystal waveguide. *arXiv*: 1401.0367 (2014).

Acknowledgments

Author contributions

W.T., L.C. and H.Q.L. conceived the idea. W.T. designed the photonic model and carried out electromagnetic calculation. L.C. carried out calculation for effective Hamiltonian and winding number. X.J. carried out FDFD simulation. L.C. and H.Q.L. provided theoretical analysis and interpretation. All authors co-wrote the paper.

Additional information

Competing financial interests: The authors declare no competing financial interests.

How to cite this article: Tan, W., Chen, L., Ji, X. & Lin, H.-Q. Photonic simulation of topological superconductor edge state and zero-energy mode at a vortex. *Sci. Rep.* **4**, 7381; DOI:10.1038/srep07381 (2014).